Cooperative Spectrum Sensing: A Blind and Soft Fusion Detector

Jingwen Tong, Ming Jin, Qinghua Guo, *Member, IEEE*, and Youming Li

***Abstract*— Cooperative spectrum sensing has been studied to combat the hidden terminal problem by exploiting the spatial diversity in cognitive radio (CR) networks. This paper concerns blind cooperative spectrum sensing with soft fusion, where the *a priori* knowledge of channels and primary signals is unavailable, and soft information is transmitted from each secondary user (SU) to a fusion center for detection. We first introduce the Quade test to design a blind detector. Then, a new detector with both lower computational complexity and lower overhead is derived, where only the estimated power and the variance of the instantaneous power at each SU are required at the fusion center. The analytical expressions for the detection performance, in terms of false-alarm probability and detection probability, are derived for the proposed detector. Simulation results are provided to validate the theoretical analyses and demonstrate the superior performance of proposed detector compared to the state-of-the-art detectors. It is also shown that, with the increase of the number of hidden terminals in the CR, the proposed detector can maintain high detection performance while the conventional detectors exhibit rapid performance degradation.**

***Index Terms*— Cognitive radio, cooperative spectrum sensing, soft fusion, blind detection.**

I. Introduction

DUE to the explosively increasing demands for radio spectrum resources, the static spectrum allocation policy faces the challenge of spectrum scarcity [1], [2]. Cognitive radio (CR) allows secondary users (SUs) to opportunistically access the idle frequency bands allocated to primary users (PUs), and is promising to tackle the challenge [3]–[5]. To probe available spectrum holes and avoid unacceptable interference to PUs, SUs need to sense the activities of PUs reliably. Hence, spectrum sensing plays a key role in CR networks [6].

In non-cooperative spectrum sensing, spectrum sensing is performed at a single SU to make a decision on the presence of primary signals [7]. A variety of non-cooperative spectrum sensing techniques have been proposed, such as the energy detection (ED) [8], [9], cyclostationary detection [10], compressive sensing detection [11], pilot/cyclic-prefix based detection [12]–[14] and covariance matrix-based detection (including covariance absolute value and eigenvalue-based detectors) [15]–[19]. However, non-cooperative spectrum sensing may suffer from the hidden terminal problem due to deep fading and shadowing effects, resulting in unreliable sensing performance [20].

Taking advantage of the spatial diversity by deploying multiple distributed SUs, cooperative spectrum sensing is able to effectively overcome the hidden terminal problem, and it has become an important option in CR networks. Some of the above mentioned detectors can be directly applied to cooperative spectrum sensing. For example, the eigenvalue-based detectors (including the maximum-minimum eigenvalue (MME) detector [17], the arithmetic-to-geometric mean (AGM) detector [18] and the maximum-to-arithmetic mean (MAM) detector [19]) can be used to perform cooperative spectrum sensing at the fusion center based on the signal samples transmitted from all SUs. However, the transmission of data from SUs to the fusion center leads to high overhead. To reduce the overhead, different fusion approaches have been proposed by transmitting only a small amount of sensing data to the fusion center. The fusion approaches can be mainly categorized into hard fusion and soft fusion [21]–[23]. In hard fusion, each SU first makes a local decision based on its own recorded data, and then transmits its local decision to the fusion center. After collecting all local decisions from SUs, the fusion center makes a final decision on the presence/absence of primary signals. Considering that conventional binary local decision may induce a large amount of information loss, Shah *et al.* [21] and So and Sung [22] investigated hard fusion based on multi-bit quantized local decisions. It was pointed out that the degree of difficulty for designing a hard fusion approach will increase quickly with the bit number for quantization, and two-bit local decisions are often taken in practice [21], [22]. Hence, hard fusion may result in inferior performance compared to soft fusion.

The current focus of soft fusion is mainly on weighting estimated power values collected from SUs, and optimal weighting coefficients were designed for different kinds of channels [23], [23]–[29]. In [23], a modified deflection coefficient based linear fusion approach was proposed for slow fading channels. In [24], an optimal soft fusion rule was derived under the assumptions of Gaussian primary signals and known signal-to-noise ratios (SNRs). It was further shown that

Manuscript received August 8, 2017; revised November 21, 2017 and January 26, 2018; accepted January 31, 2018. Date of publication February 9, 2018; date of current version April 8, 2018. This work was supported in part by the National Natural Science Foundation of China under Grant 61301152 and Grant 61571250, in part by the Australian Research Councils DECRA under Grant DE120101266, in part by the Zhejiang Natural Science Foundation under Grant LY18F010008, and in part by the K. C. Wong Magna Fund from Ningbo University. The associate editor coordinating the review of this paper and approving it for publication was E. A. Jorswieck. *(Corresponding author: Ming Jin.)*

J. Tong, M. Jin, and Y. Li are with the Faculty of Electrical Engineering and Computer Science, Ningbo University, Ningbo 315211, China (e-mail: jwentong0203@qq.com; jinming@nbu.edu.cn; liyouming@nbu.edu.cn).

Q. Guo is with the School of Electrical, Computer and Telecommunications Engineering, University of Wollongong, Wollongong, NSW 2522 Australia (e-mail: qguo@uow.edu.au).

Color versions of one or more of the figures in this paper are available online at http://ieeexplore.ieee.org.

Digital Object Identifier 10.1109/TWC.2018.2801833

the equal gain combining (EGC) [25] and the maximal ratio combining (MRC) fusion rules are near-optimal at high and low SNRs, respectively. With the assumption of deterministic but unknown primary signals, an optimal soft fusion rule was derived in [23] and [26]. However, these rules require the statistical characteristics of the received power under both hypotheses. In [27], an average likelihood ratio detector was derived under flat fading channels, in which the Nakagami-*m* and log-normal distributions were used to model the small- and large-scale fadings, respectively. However, this detector requires the statistical distributions of the small- and large-scale fadings. In [28], optimal and sub-optimal soft fusion rules were derived for fast Rayleigh fading channels with known distributions, where the channel gains due to the large-scale fading are assumed to be known. In [29], an optimal fusion rule based on the likelihood ratio test was proposed for block-fading channels, where the Nakagami-*m* distribution was used to model the small-scale fading and the channel gains due to the large-scale fading are assumed to be known. This rule was re-investigated for the case of Rayleigh small-scale fading channels in [30]. In summary, all the above soft fusion rules except the EGC require the *a priori* statistical knowledge of channels from PU to SUs. The acquisition of the *a priori* knowledge will impose additional burdens to SUs and sometimes it may be difficult or even impractical to acquire the knowledge, e.g., in the scenario that the channel gains are time varying. Although EGC does not require the *a priori* knowledge of channels, it needs the noise power to set the decision threshold. Hence, EGC is a semi-blind detector and its performance can degrade severely under noise uncertainty [31].

In this paper, we assume that the *a priori* knowledge of channels and primary signals is unavailable, and develop a blind soft fusion detector. Although the *a priori* knowledge of channel gains is unknown, we assume that the channel gains from a PU to SUs are different due to spatial diversity. It is assumed that the signals undergo channels with small- and large-scale fadings, and the channel gains due to large-scale fading keep constant within a sensing duration, while the channel gains due to small-scale fading may be time-varying within a sensing duration. The differences of this work compared to existing ones and the main contributions are summarized in the following.

- We consider soft fusion detection for cooperative spectrum sensing with the assumption that the *a priori* knowledge of channels and primary signals is unavailable, where the existing soft fusion approaches (except EGC) are not applicable.
- We first develop a Quade test-based blind cooperative sensing detector with soft fusion. To the best of our knowledge, it is the first time to introduce the Quade test to the field of spectrum sensing. To reduce the computational complexity, we then devise a new detector, which delivers significantly improved performance but with much lower complexity compared to the Quade test-based one.
- As the new detector still involves high overhead due to the requirement of data transmission from SUs to the fusion center, we step further and propose an equivalent detector, which only requires the power and variance of instantaneous power at each SU, leading to a significant reduction in overhead.
- We show that, with the increase of the number of hidden terminals, the conventional cooperative spectrum sensing detectors exhibit rapid performance degradation. In contrast, our proposed detector can maintain high detection performance.

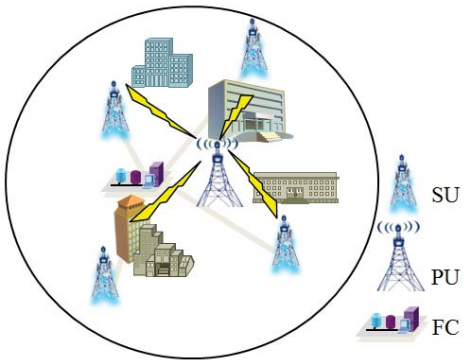

Fig. 1. Cognitive radio network for spectrum sensing.

The remainder of this paper is organized as follows. The signal model is introduced in Section II. In Section III, the Quade test is employed to implement blind cooperative spectrum sensing, and an analytical expression for the false-alarm probability is derived. In Section IV, we propose a new blind cooperative detector and derive theoretical expressions for its false-alarm probability and detection probability. Simulation results are presented in Section V and concluding remarks are made in Section VI.

Notation: $\mathbb{E}[\cdot]$ and $\mathbb{V}[\cdot]$ represent the expectation and variance operators, respectively. $\ln(\cdot)$ denotes the natural logarithm, $\Gamma(\cdot)$ denotes the Gamma function, $B(\cdot,\cdot)$ denotes the beta function, and $B(\cdot;\cdot,\cdot)$ denotes the incomplete beta function. $\mathbb{R}(\cdot)$ denotes the real part of a number, and $(\cdot)^*$ is the conjugate operator. $\mathcal{CN}(a,b)$ represents a proper complex Gaussian distribution with mean a and variance b, $\mathcal{N}(c,d)$ represents a real Gaussian distribution with mean c and variance d, Gamma (α,β) represents a gamma distribution with a shape parameter α and a scale parameter β, and Beta (α,β) represents a beta distribution with shape parameters α and β. Let $\mathcal{H}_0$ represent the null hypothesis, i.e., PUs are inactive, and $\mathcal{H}_1$ represent the alternative hypothesis, i.e., PUs are active. The false-alarm probability P_f is defined as Prob(Reject $\mathcal{H}_0|\mathcal{H}_0$ is true) where Prob$(\cdot)$ represents the probability of an event. The detection probability P_d is defined as Prob(Accept $\mathcal{H}_1|\mathcal{H}_1$ is true), and the miss-detection probability P_m is defined as $1-P_d=$ Prob(Reject $\mathcal{H}_1|\mathcal{H}_1$ is true).

II. Signal Model

We consider a CR network in Fig. 1, where L distributed SUs are deployed uniformly within the coverage of a PU. The CR network is allowed to opportunistically access the idle channel which is allocated to the PU. To avoid interfering PU

receivers which may be located within the coverage of the CR network, the CR network needs to perform spectrum sensing before accessing the channel. In cooperative spectrum sensing, SUs sent their information to the fusion center through a dedicated channel, and the fusion center makes a final decision on the presence/absence of primary signals. So, we have the following binary hypotheses: $\mathcal{H}_1$ representing that the PU is active, and $\mathcal{H}_0$ representing that the PU is inactive.

Assume that each SU obtains K samples within a sensing duration. With the above binary hypotheses, the kth ($k = 1, 2, \cdots, K$) sample at the lth ($l = 1, 2, \cdots, L$) SU is given by

$$x_l(k) = \begin{cases} n_l(k), & \mathcal{H}_0 \\ h_l(k)\sqrt{g_l}s_l(k) + n_l(k), & \mathcal{H}_1 \end{cases} \tag{1}$$

where $n_l(k)$ denotes the additive independent and identically distributed (i.i.d.) circularly symmetric complex Gaussian noise with mean zero and variance σ_n^2, i.e., $n_l(k) \sim \mathcal{CN}(0, \sigma_n^2)$; $s_l(k) = s(k - \tau_l)$ denotes the received primary signal at the lth SU with a time delay of τ_l and the transmitted primary signal $s(k)$ is assumed to be Gaussian distributed with mean zero and variance σ_s^2, i.e., $s(k) \sim \mathcal{CN}(0, \sigma_s^2)$; g_l denotes the power gain due to large-scale fading and $h_l(k)$ denotes the small-scale fast fading channel from the PU to the lth SU. It is assumed that g_l is time-invariant during a sensing duration, and the primary signals and the channel gains are independent of each other. Considering that the SUs are distributively deployed to overcome the hidden terminal problem, we assume that g_l follows a log-normal distribution, i.e., the probability density function (PDF) of g_l is given by [32]

$$f_{g_l}(u) = \frac{1}{u\sqrt{2\pi}\sigma} e^{-\frac{(\ln u - \mu)^2}{2\sigma^2}} \tag{2}$$

where μ (in dB) and σ (in dB) are the mean and standard deviation of $\ln g_l$. In addition, we assume Nakagami-m small-scale fading channels. Let $h_l(k) = |h_l(k)|e^{j2\pi\theta}$ where θ is uniformly distributed on [0, 1) and the PDF of $|h_l(k)|$ is given by

$$f_{|h_l(k)|}(u) = \frac{1}{\left(\frac{\Omega}{m}\right)^m \Gamma(m)} u^{m-1} e^{-\frac{u}{\Omega/m}} \tag{3}$$

with Ω being the average power gain of the Nakagami-m channels and $m \geq 0.5$. It is well known that the Rayleigh and one-sided Gaussian distributions are the special cases of the PDF in (3) with $m = 1$ and $m = 0.5$, respectively.

Let $e_{l,k}$ be the instantaneous power of the received signal at the kth time instant of the lth SU, i.e.,

$$e_{l,k} = |x_l(k)|^2. \tag{4}$$

Thus, the CR network has a total of LK instantaneous power values in a sensing duration. Arrange the LK instantaneous power values in a matrix as

$$\mathbf{P} = \begin{bmatrix} e_{1,1} & e_{1,2} & \cdots & e_{1,K} \\ e_{2,1} & e_{2,2} & \cdots & e_{2,K} \\ \vdots & \vdots & \ddots & \vdots \\ e_{L,1} & e_{L,2} & \cdots & e_{L,K} \end{bmatrix} \tag{5}$$

where the lth row are the instantaneous power values from the lth SU.

III. Quade Test-Based Cooperative Spectrum Sensing

The Quade test is a non-parametric test for heterogeneity among multiple treatments [33]. The spatial diversity in cooperative spectrum sensing leads to heterogeneity among the powers at different SUs, which can be detected with the Quade test. In this Section, we introduce the Quade test to the field of spectrum sensing, develop a Quade test-based detector for cooperative sensing, and analyze its performance.

A. Quade Test-Based Detector

After collecting all the LK instantaneous power values from the SUs (i.e., the power matrix $\mathbf{P}$ is available), the fusion center can perform detection with the Quade test-based detector as detailed in the following. Firstly, rank the elements along each column in $\mathbf{P}$, which gives a rank matrix $\mathbf{R}$ as

$$\mathbf{R} = \begin{bmatrix} r_{1,1} & r_{1,2} & \cdots & r_{1,K} \\ r_{2,1} & r_{2,2} & \cdots & r_{2,K} \\ \vdots & \vdots & \ddots & \vdots \\ r_{L,1} & r_{L,2} & \cdots & r_{L,K} \end{bmatrix}. \tag{6}$$

Take the kth columns of $\mathbf{P}$ and $\mathbf{R}$ as an example. If the instantaneous power $e_{l,k}$ in $\mathbf{P}$ is the pth largest one among $\{e_{1,k}, e_{2,k}, \cdots, e_{L,k}\}$, then $r_{l,k}$ in $\mathbf{R}$ takes on the value of the integer p. In other words, the vector $[r_{1,k}, r_{2,k}, \cdots, r_{L,k}]$ is a permutation of the integer vector $[1, 2, \cdots, L]$. Then, the kth column of $\mathbf{R}$ is weighted by a coefficient $q_k \in [1, K]$. The value of q_k is determined so that $\max\limits_l e_{l,k} - \min\limits_l e_{l,k}$ is the q_kth largest one among $\{\max\limits_l e_{l,1} - \min\limits_l e_{l,1}, \max\limits_l e_{l,2} - \min\limits_l e_{l,2}, \cdots, \max\limits_l e_{l,K} - \min\limits_l e_{l,K}\}$. It can be shown that q_k is independent of the elements in $\mathbf{R}$ due to the ranking operation [33]. Subtracting the mean of $r_{l,k}$ of $\mathbf{R}$, i.e.,

$$\bar{r} = \frac{1}{LN}\sum_{l=1}^{L}\sum_{k=1}^{K} r_{l,k} = \frac{L+1}{2}, \tag{7}$$

and weighting the kth column with q_k, we obtain that

$$\mathbf{Z} = \begin{bmatrix} z_{1,1} & z_{1,2} & \cdots & z_{1,K} \\ z_{2,1} & z_{2,2} & \cdots & z_{2,K} \\ \vdots & \vdots & \ddots & \vdots \\ z_{L,1} & z_{L,2} & \cdots & z_{L,K} \end{bmatrix} \tag{8}$$

where

$$z_{l,k} = q_k(r_{l,k} - \bar{r}). \tag{9}$$

Finally, the test-statistic of the Quade test-based detector is given by [33]

$$T_{\text{Quade}} = (K-1)\frac{Z_1}{Z_2 - Z_1} \tag{10}$$

where

$$Z_1 = \frac{1}{K}\sum_{l=1}^{L}\left(\sum_{k=1}^{K} z_{l,k}\right)^2 \tag{11}$$

and

$$Z_2 = \sum_{l=1}^{L}\sum_{k=1}^{K} z_{l,k}^2 \tag{12}$$

can be regarded as the variances of weighted ranks. By comparing T_{Quade} with a given decision threshold λ, the decision on the presence or absence of primary signals can be made.

Now, we explain the rationale behind the test-statistic T_{Quade}. It can be obtained that Z_2 in (10) is a constant no matter whether primary signals are present or not. Under $\mathcal{H}_0$, the instantaneous powers $\{e_{l,k}\}$ at all SUs are i.i.d. Because the probability that continuous random variables are equal is zero, we can obtain that $r_{l,k}$ (which is the rank of $e_{l,k}$) is uniformly distributed over the integer set $[1, L]$ and $\bar{r} = (L+1)/2$ under $\mathcal{H}_0$. Hence, due to the independence between q_k and $r_{l,k}$, we have

$$\mathbf{E}[z_{l,k}|\mathcal{H}_0] = \mathbf{E}[q_k]\mathbf{E}[r_{l,k} - \bar{r}] = 0 \tag{13}$$

which means that Z_1 is close to zero under $\mathcal{H}_0$. Under $\mathcal{H}_1$, $r_{l,k}$ is no longer uniformly distributed because of the non-identical distributions of $\{e_{l,k}\}$ among different SUs, thus

$$\mathbf{E}[z_{l,k}|\mathcal{H}_1] \neq 0. \tag{14}$$

Because $\{e_{l,k}, \forall k\}$ are i.i.d., $\{r_{l,k}, \forall k\}$ are also i.i.d. Hence, the mean of $r_{l,k} - \bar{r}$ is independent of k. In addition, q_k is larger than zero. Thus, $\{\mathbf{E}[z_{l,k}|\mathcal{H}_1], \forall k\}$ are either all positive or all negative under $\mathcal{H}_1$. Therefore, $(\sum_{k=1}^{K} z_{l,k})^2$ is statistically larger under $\mathcal{H}_1$ than under $\mathcal{H}_0$, and Z_1 is statistically larger under $\mathcal{H}_1$ than under $\mathcal{H}_0$. Therefore, the test-statistic T_{Quade} in (10) can be used to discriminate the hypotheses $\mathcal{H}_0$ and $\mathcal{H}_1$.

B. False-Alarm Probability and Decision Threshold

We give analytical expressions for the false-alarm probability and decision threshold of the Quade test-based detector. They can be derived based on the following proposition in [34].

Proposition 1 (See [34], Sec. 6.3.4): The test-statistic T_{Quade} in (10) asymptotically follows the $\mathcal{F}$-distribution with degrees of freedom (DoF) of $L-1$ and $(L-1)(K-1)$ under $\mathcal{H}_0$, i.e.,

$$T_{\text{Quade}} \sim \mathcal{F}_{d_1,d_2} \tag{15}$$

where $\mathcal{F}_{d_1,d_2}$ denotes the $\mathcal{F}$-distribution with DoF of $d_1 = L-1$ and $d_2 = (L-1)(K-1)$.

With ***Proposition 1***, we can obtain that the analytical expression of false-alarm probability with a given decision threshold λ is given by

$$P_f = 1 - I_{\frac{d_1\lambda}{d_1\lambda+d_2}}\left(\frac{d_1}{2}, \frac{d_2}{2}\right) \tag{16}$$

where $I_u(a,b)$ is the regularized incomplete beta function

$$I_u(a,b) = \frac{B(u;a,b)}{B(a,b)}, \tag{17}$$

with $B(u;a,b)$ being the incomplete beta function

$$B(u;a,b) = \int_0^u t^{a-1}(1-t)^{b-1}dt \tag{18}$$

and $B(a,b)$ being the beta function

$$B(a,b) = \int_0^1 t^{a-1}(1-t)^{b-1}dt. \tag{19}$$

The analytical expression of decision threshold with a given false-alarm probability P_f is given by

$$\lambda = \frac{d_1+d_2}{d_1} B^{-1}\left((1-P_f)B\left(\frac{d_1}{2}, \frac{d_2}{2}\right), \frac{d_1}{2}, \frac{d_2}{2}\right) \tag{20}$$

where $B^{-1}\left(\cdot, \frac{d_1}{2}, \frac{d_2}{2}\right)$ denotes the inverse function of $B\left(\cdot, \frac{d_1}{2}, \frac{d_2}{2}\right)$.

IV. New Blind Cooperative Spectrum Sensing and Its Performance Analysis

The Quade test-based cooperative spectrum sensing involves high computational complexity due to the ranking operations. Moreover, the original instantaneous power values are not used in the Quade test, inducing certain performance loss. To overcome the above drawbacks, we propose a new blind detector for cooperative spectrum sensing. First, the ranking operation is removed and the instantaneous power values at SUs are directly employed, which can potentially improve the detection performance while reducing the computational complexity. Second, it was pointed out in [33] and [35] that it is grossly inefficient to use the weighting when ranking operations are not taken, and we can significantly reduce the overhead of reporting local data from SUs to the fusion center by removing the weighting operations. The above will lead to a new detector with better performance and lower computational complexity and overhead. It will be shown in Section V that the new detector outperforms the Quade test-based one, and even delivers a better performance than the ideal EGC (i.e., EGC with exact noise power).

A. New Detector

Following the idea of the Quade test and replacing the ranks $r_{l,k}$ in (10) with the corresponding power $e_{l,k}$, we can obtain a detector whose test-statistic is given by

$$T_w = (K-1)\frac{\Theta_1}{\Theta_2 - \Theta_1} \tag{21}$$

where

$$\Theta_1 = \frac{1}{K}\sum_{l=1}^{L}\left(\sum_{k=1}^{K}\epsilon_{l,k}\right)^2 \tag{22}$$

and

$$\Theta_2 = \sum_{l=1}^{L}\sum_{k=1}^{K}\epsilon_{l,k}^2 \tag{23}$$

with

$$\epsilon_{l,k} = w_k\left(e_{l,k} - \frac{1}{LK}\sum_{l=1}^{L}\sum_{k=1}^{K} e_{l,k}\right) \tag{24}$$

and

$$w_k = \max_l e_{l,k} - \min_l e_{l,k}. \tag{25}$$

In the Quade test, the weighting factor q_k was introduced to compensate the information loss caused by the use of the ranks (rather than the original power values) [33]. As we are using the instantaneous power values directly in building our test-statistic, we may remove the weighting factor w_k in (21), leading to a new detector

$$T_{\text{proposed}} = (K-1)\frac{S_1}{S_2 - S_1} \tag{26}$$

where

$$S_1 = \frac{1}{K}\sum_{l=1}^{L}\left(\sum_{k=1}^{K} s_{l,k}\right)^2 \tag{27}$$

and

$$S_2 = \sum_{l=1}^{L}\sum_{k=1}^{K} s_{l,k}^2 \tag{28}$$

with

$$s_{l,k} = e_{l,k} - \frac{1}{LK}\sum_{l=1}^{L}\sum_{k=1}^{K} e_{l,k}. \tag{29}$$

From the expression of T_{proposed} in (26), we find that the fusion center still requires all $e_{l,k}$ from SUs. Thus, this detector has the same overhead of data transmission from SUs to the fusion center as the Quade test-based detector. To reduce the overhead, we derive an equivalent one for the detector in (26).

By the Cauchy-Schwarz inequality, we have

$$\left(\sum_{k=1}^{K} s_{l,k}\right)^2 \le K\sum_{k=1}^{K} s_{l,k}^2. \tag{30}$$

Because the elements in $\{s_{l,k}\}$ are continuous random variables, the probability that the left term equals the right one in (30) is zero. Hence,

$$\left(\sum_{k=1}^{K} s_{l,k}\right)^2 < K\sum_{k=1}^{K} s_{l,k}^2 \tag{31}$$

and then

$$0 < S_1 < S_2. \tag{32}$$

Eq. (32) gives that

$$0 < \frac{S_1}{S_2} < 1. \tag{33}$$

Thus,

$$\begin{aligned} T_{\text{proposed}} &= (K-1)\frac{S_1}{S_2 - S_1} \\ &= (K-1)\frac{\frac{S_1}{S_2}}{1 - \frac{S_1}{S_2}} \end{aligned} \tag{34}$$

is a monotone increasing function with respect to S_1/S_2. Therefore, the detector T_{proposed} in (26) is equivalent to

$$T_{\text{proposed}} = \frac{S_1}{S_2} = \frac{\frac{1}{K}\sum_{l=1}^{L}\left(\sum_{k=1}^{K} s_{l,k}\right)^2}{\sum_{l=1}^{L}\sum_{k=1}^{K} s_{l,k}^2}. \tag{35}$$

After some manipulations, the test-statistic in (35) can be further rewritten as (36), shown at the bottom of this page. Let

$$\hat{m}_{e_l} = \frac{1}{K}\sum_{k=1}^{K} e_{l,k} \tag{37}$$

be the estimated power at the lth SU, and

$$\hat{v}_{e_l}^2 = \frac{1}{K}\sum_{k=1}^{K}\left(e_{l,k} - \hat{m}_{e_l}\right)^2 \tag{38}$$

be the estimated variance of the instantaneous power at the lth SU. By using (37) and (38), the test-statistic in (36) can be rewritten as

$$T_{\text{proposed}} = \frac{\sum_{l=1}^{L}\left(\hat{m}_{e_l} - \frac{1}{L}\sum_{l=1}^{L}\hat{m}_{e_l}\right)^2}{\sum_{l=1}^{L}\hat{v}_{e_l}^2 + \sum_{l=1}^{L}\left(\hat{m}_{e_l} - \frac{1}{L}\sum_{l=1}^{L}\hat{m}_{e_l}\right)^2}. \tag{39}$$

It can be observed from (39) that, to calculate T_{proposed} at the fusion center, only two parameters (i.e., $\hat{m}_{e_l}$ and $\hat{v}_{e_l}^2$) are required to be transmitted from the lth SU. This significantly reduces the overhead of data transmission from SUs to the fusion center.

There are mainly three differences between the proposed detector and the Quade test-based detector in (10) as summarized in the following.

- No ranking operation is required by the proposed detector, which leads to lower computational complexity;
- The overhead of data transmission is significantly reduced by using the proposed detector in (39);
- In (10), Z_2 is a constant, while in (35), S_2 is a random variable. This increases the difficulty in theoretical performance analysis of the proposed detector.

B. False-Alarm and Detection Probabilities

In the following, we derive analytical expressions for the false-alarm and detection probabilities of the proposed detector in (39).

Proposition 1: The detector T_{proposed} in (39) under $\mathcal{H}_0$ approximately follows a beta distribution as

$$T_{\text{proposed}}|\mathcal{H}_0 \sim \text{Beta}\left(\frac{L-1}{2}, \frac{L(K-1)}{2}\right). \tag{40}$$

$$T_{\text{proposed}} = \frac{\sum_{l=1}^{L}\left(\frac{1}{K}\sum_{k=1}^{K} s_{l,k}\right)^2}{\frac{1}{K}\sum_{l=1}^{L}\sum_{k=1}^{K}\left(s_{l,k} - \frac{1}{K}\sum_{k=1}^{K} s_{l,k}\right)^2 + \sum_{l=1}^{L}\left(\frac{1}{K}\sum_{k=1}^{K} s_{l,k}\right)^2}. \tag{36}$$

Proof: See Appendix A. □

Base on ***Proposition*** *2*, we can obtain that the PDF of $T_{\text{proposed}}|\mathcal{H}_0$ is given by

$$f_{T_{\text{proposed}}|\mathcal{H}_0}(u) = \frac{1}{B\left(\frac{L-1}{2}, \frac{L(K-1)}{2}\right)} u^{\frac{L-3}{2}} (1-u)^{\frac{L(K-1)-2}{2}} \quad (41)$$

with $0 \leq u \leq 1$. The corresponding cumulative distribution function is given by

$$F_{T_{\text{proposed}}|\mathcal{H}_0}(u) = I_u\left(\frac{L-1}{2}, \frac{L(K-1)}{2}\right), \quad (42)$$

and thus the false-alarm probability for a given decision threshold λ reads

$$P_f = 1 - F_{T_{\text{proposed}}|\mathcal{H}_0}(\lambda). \quad (43)$$

Proposition 2: With sufficiently large K and L, the detector T_{proposed} in (39) under $\mathcal{H}_1$ approximately follows a beta distribution as

$$T_{\text{proposed}}|\mathcal{H}_1 \sim \text{Beta}\,(\alpha_1, \beta_3) \quad (44)$$

where

$$\alpha_1 = \frac{L-1}{2} \quad (45)$$

and

$$\beta_3 = \alpha_1 \left(\frac{1}{m_T} - 1\right) \quad (46)$$

with

$$m_T = \left(\frac{\beta_2^{\mathcal{H}_1}}{\beta_1^{\mathcal{H}_1}}\right)^{\alpha_1} \frac{B(\alpha_2, \alpha_1+1)}{B(\alpha_1, \alpha_2)} \times {}_2F_1\left(\alpha_1+\alpha_2, \alpha_1+1; \alpha_1+\alpha_2+1; 1-\frac{\beta_2^{\mathcal{H}_1}}{\beta_1^{\mathcal{H}_1}}\right), \quad (47)$$

α_2, $\beta_1^{\mathcal{H}_1}$ and $\beta_2^{\mathcal{H}_1}$ being respectively given in (A.11), (B.20) and (B.21), and ${}_2F_1(\cdot,\cdot;\cdot;\cdot)$ denoting the hypergeometric function [39].

Proof: See Appendix B. □

Base on ***Proposition*** *3*, we can obtain that the PDF of $T_{\text{proposed}}|\mathcal{H}_1$ is given by

$$f_{T_{\text{proposed}}|\mathcal{H}_1}(u) = \frac{1}{B\,(\alpha_1, \beta_3)} u^{\alpha_1-1}(1-u)^{\beta_3-1} \quad (48)$$

with $0 \leq u \leq 1$. Finally, the detection probability for a given decision threshold λ reads

$$P_d = 1 - F_{T_{\text{proposed}}|\mathcal{H}_1}(\lambda) \quad (49)$$

where

$$F_{T_{\text{proposed}}|\mathcal{H}_1}(u) = I_u\,(\alpha_1, \beta_3)\,. \quad (50)$$

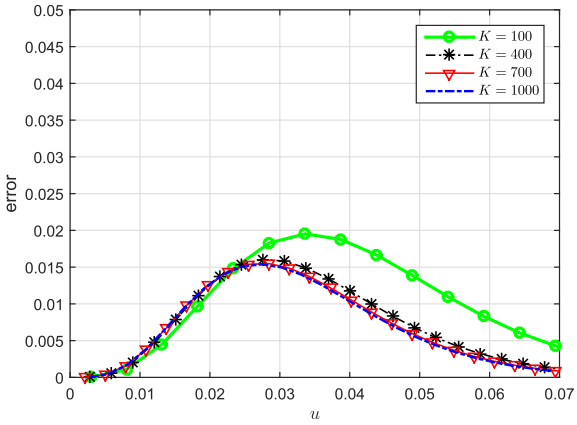

Fig. 2. The approximation error with respect to u where the term K varying from 100 to 1000.

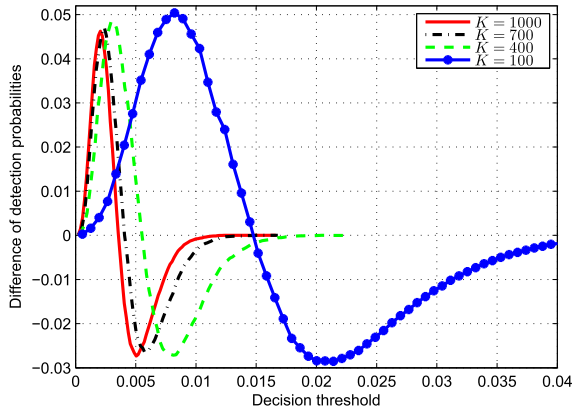

Fig. 3. Differences of the detection probabilities obtained by using the theoretical expression in (50) and Monte Carlo simulation for difference K when $L = 10$ and SNR$= -16$dB.

V. Simulations and Discussions

In this section, numerical simulation results are provided to verify the theoretical analyses and evaluate the performance of the proposed detector. In all simulations, the channel parameters $\mu = 0$dB, $10\sigma/\ln 10 = 12$dB, $\Omega = 1$ for $m = 0.5$ and $m = 1$, where $m = 0.5$ represents one side Gaussian fading channels and $m = 1$ represents Rayleigh fading channels.

First, we evaluate the approximation error between $I_u\,(\alpha_1, \beta_3)$ in (50) and the cumulative distribution function (CDF) from (B.22), i.e.,

$$\text{error}(u) = I_u\,(\alpha_1, \beta_3) - \int_0^u f_{T_{\text{proposed}}|\mathcal{H}_1}(x)dx. \quad (51)$$

Fig. 2 shows the approximation error with respect to u where $L = 10$, SNR$= -16$dB, $\mu = 0$dB, $10\sigma/\ln 10 = 12$dB, $\Omega = 1$ and $m = 0.5$ for different K. It can be observed from Fig. 2 that the approximation error decreases when K increases, and the maximum approximation error is less than 0.02 even when $K = 100$.

Considering that there also exists approximation error in deriving $f_{T_{\text{proposed}}|\mathcal{H}_1}(u)$ in (B.22), in the following, we directly compare the theoretical expression in (50) with the Monte Carlo simulation results of detection probability of the proposed detector for different K. Fig. 3 shows the differences between the detection probabilities obtained by using the

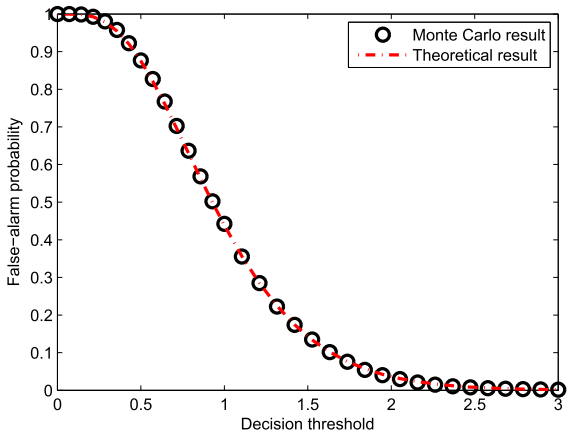

Fig. 4. Theoretical and simulation results for the false-alarm probability of the Quade test-based detector where $L = 10$ and $K = 1000$.

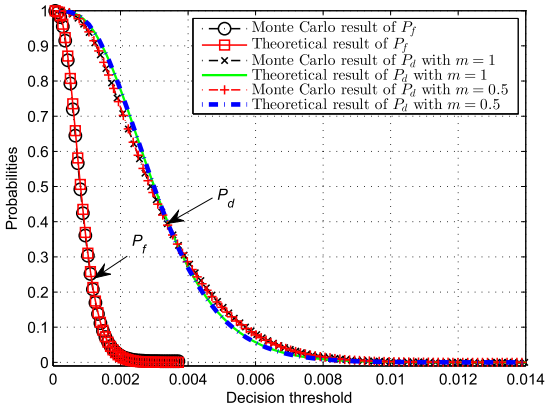

Fig. 5. Theoretical and Monte Carlo simulation results for the false-alarm and detection probabilities of the proposed detector when $L = 10$, $K = 1000$ and SNR$= -16$dB.

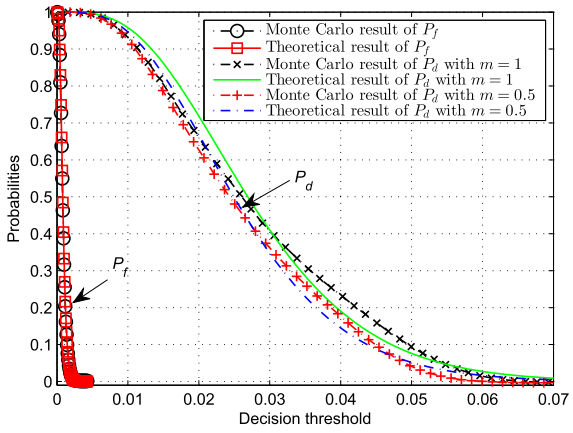

Fig. 6. Theoretical and Monte Carlo simulation results for the false-alarm and detection probabilities of the proposed detector when $L = 10$, $K = 1000$ and SNR$= -10$dB.

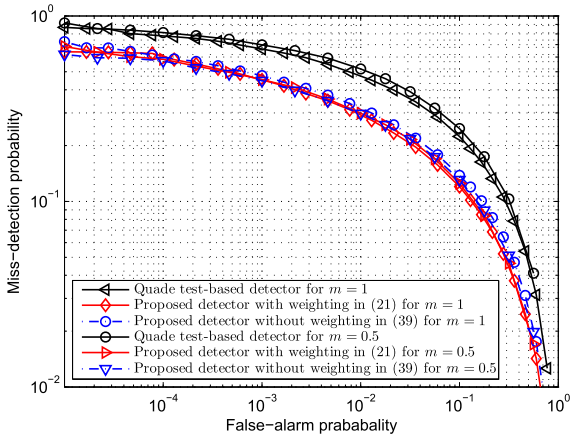

Fig. 7. ROC curves for the Quade test-based detector, the proposed detector with weighting coefficients in (21) and the proposed detector without weighting coefficients in (39) when $L = 10$, $K = 1000$ and SNR $= -16$dB.

theoretical expression in (50) and Monte Carlo simulation for different K when $L = 10$, SNR$= -16$dB, $\mu = 0$dB, $10\sigma/\ln 10 = 12$dB, $\Omega = 1$ and $m = 0.5$. It can be observed that the maximum difference is only about 0.05 when $K \geq 100$. This implies that the approximation error is small by using (50) to evaluate the detection probability of the proposed detector.

Fig. 4 shows the theoretical and simulation results for the false-alarm probability of the Quade test-based detector where $L = 10$ and $K = 1000$. It can be seen that the theoretical result from (15) matches the Monte Carlo simulation result well.

Fig. 5 shows the theoretical and Monte Carlo simulation results for the false-alarm and detection probabilities of the proposed detector when $L = 10$, $K = 1000$ and SNR $= -16$dB. The theoretical results for false-alarm and detection probabilities are obtained by using (43) and (49), respectively. It can be observed that the theoretical result for the false-alarm probability matches the Monte Carlo simulation result quite well. A slight difference is found between the theoretical and Monte Carlo results for the detection probability, which is due to the approximations used in the derivation. In addition, Fig. 5 shows that the performance difference of the proposed detector for one-sided Gaussian and Rayleigh fading channels is very small. Fig. 6 shows the theoretical and Monte Carlo simulation results for the false-alarm and detection probabilities by increasing SNR to -10dB. The results validate the theoretical results again.

Fig. 7 shows the receiver operating characteristic (ROC) curves for the Quade test-based detector, the proposed detector with weighting coefficients in (21) and the proposed detector without weighting coefficients in (39) when $L = 10$, $K = 1000$ and SNR $= -16$dB. It can be observed that the proposed detectors with and without weighting coefficients have similar detection performance. This verifies that the weighting operation has a negligible impact on the detection performance (but obtaining the weighting coefficients will give rise to additional computational complexity and overhead in the CR network). Moreover, Fig. 7 shows that the proposed detectors significantly outperform the Quade test-based detector.

In the following, we evaluate the performance of the proposed detector in (39) by comparing it with existing cooperative spectrum sensing detectors (including three eigenvalue-based detectors and the EGC detector). The reason that we choose the eigenvalue-based detectors and the EGC detector

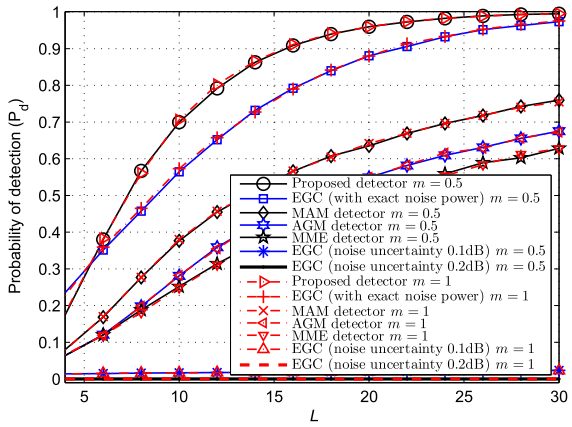

Fig. 8. Detection probabilities versus the number of SUs L for various detectors when SNR $= -16$dB and $K = 1000$ at $P_f = 0.01$.

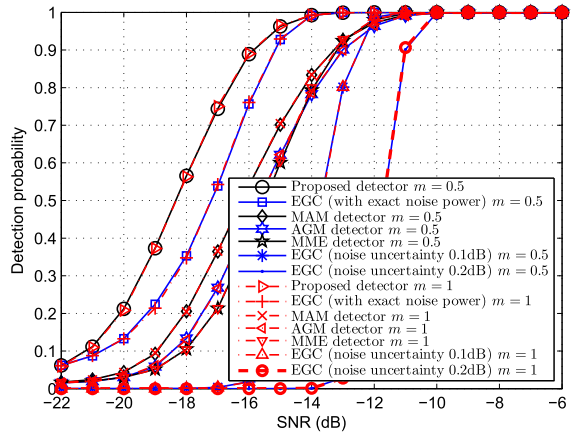

Fig. 9. Detection probabilities versus SNR for various detectors when $L = 15$ and $K = 1000$ at $P_f = 0.01$.

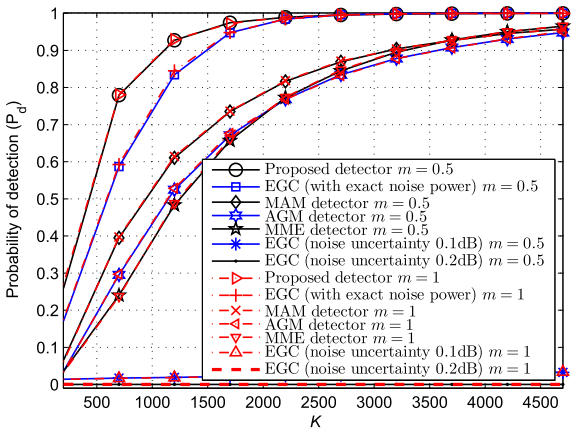

Fig. 10. Detection probabilities versus sample number K for various detectors when $L = 15$ and SNR $= -16$dB at $P_f = 0.01$.

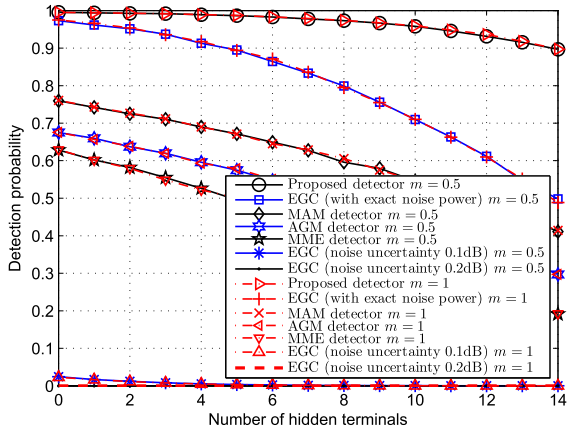

Fig. 11. Detection probability versus the number of hidden terminals when SNR $= -16$dB, $L = 30$, $K = 1000$ and $P_f = 0.01$.

is because they do not require the *a priori* knowledge of channels or primary signals.

Fig. 8 shows the detection probabilities versus the number of SUs L for various detectors when SNR $= -16$dB and $K = 1000$ at $P_f = 0.01$. It can be seen that the detection probabilities of these detectors (except the EGC under noise uncertainty) increase with the number of SUs, and the performance of the proposed detector improves faster than the other detectors. It can also be observed that the EGC is sensitive to noise uncertainty, although it outperforms the proposed detector with a small L. Note that EGC is optimal when no characteristics of signals or channels are used. However, our proposed detector exploits the spatial diversity, leading to better performance than EGC when $L \geq 6$ in Fig. 6. On the other hand, despite exploiting the spatial diversity, the proposed detector does not require the *a priori* knowledge of each channel, e.g., channel gains, so it is a blind detector.

Fig. 9 shows the detection probabilities of various detectors at different SNRs when $L = 15$, $K = 1000$ and $P_f = 0.01$. Fig. 10 shows the detection probabilities of various detectors with different K when $L = 15$ and SNR $= -16$dB at $P_f = 0.01$. It can be seen from Figs. 9 and 10 that our proposed detector outperforms the other detectors.

To evaluate the impact of hidden terminals on the detection performance of the detectors, Fig. 11 shows the detection probabilities of various detectors for different numbers of hidden terminals when SNR $= -16$dB, $L = 30$ and $K = 1000$ and $P_f = 0.01$. In the simulations, the received primary signal power is set to be zero for the hidden terminals, as the hidden terminals cannot receive any primary signals. It is observed that the proposed detector keeps a high detection performance and the other detectors degrade severely with the increase of the number of hidden terminals. When the number of hidden terminal increase from 0 to 14 (i.e., it exceeds one third of the total number of SUs), the proposed detector still has a detection probability of over 0.9, but the detection probability of ECG with exact noise power is only about 0.5. The result indicates that our proposed detector can more effectively combat the hidden terminal problem.

Fig. 12 shows the detection probabilities versus the parameter m of Nakagami-m channels for various detectors where SNR $= -16$dB, $K = 1000$, $P_f = 0.01$, $L = 30$ and the number of hidden SUs is 14. It can be seen that, when the number of hidden SUs is large, only the proposed detector can achieve satisfactory performance (the detection probability is 0.9), while other detectors perform badly (the detection probability is about or less than 0.5).

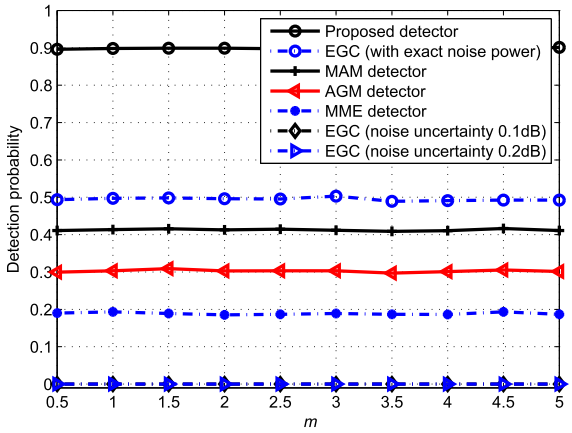

Fig. 12. Detection probability versus the parameter m where SNR $= -16$dB, $K = 1000$, $P_f = 0.01$, $L = 30$ and the number of hidden SUs is 14.

VI. Conclusion

In this work, we have introduced the Quade test to the field of spectrum sensing for blind detection in cooperative spectrum sensing. To reduce the computational complexity of the Quade test-based detector, we have proposed a new detector which avoids the ranking operations. Moreover, to reduce the overhead of data transmission in CR network, we have further developed an equivalent detector. The theoretical expressions for the false-alarm and detection probabilities of the proposed detector have been derived. Numerical simulations have verified the theoretical expressions and demonstrated that the proposed detector outperforms the existing ones and it is more effective in combating the hidden terminal problem.

Appendix A
Proof of Proposition 2

Under $\mathcal{H}_0$, the elements in $\{e_{l,k}\}$ are i.i.d. with mean σ_n^2 and variance σ_n^4. With sufficiently large K and by the central limit theorem (CLT), we can obtain that $\hat{m}_{e_l}$ follows Gaussian distribution with mean σ_n^2 and variance σ_n^4/K, i.e.,

$$\hat{m}_{e_l}|\mathcal{H}_0 \sim \mathcal{N}\left(\sigma_n^2, \frac{1}{K}\sigma_n^4\right). \tag{A.1}$$

Hence,

$$\left(\hat{m}_{e_l} - \frac{1}{L}\sum_{l=1}^{L}\hat{m}_{e_l}\right)|\mathcal{H}_0 \sim \mathcal{N}\left(0, \frac{L-1}{LK}\sigma_n^4\right) \tag{A.2}$$

and thus

$$\sum_{l=1}^{L}\left(\hat{m}_{e_l} - \frac{1}{L}\sum_{l=1}^{L}\hat{m}_{e_l}\right)^2 |\mathcal{H}_0 \sim \text{Gamma}\left(\frac{L-1}{2}, \frac{2(L-1)}{LK}\sigma_n^4\right) \tag{A.3}$$

where Gamma(α, β) denotes the gamma distribution

$$f(u) = \frac{1}{\Gamma(\alpha)\beta^{\alpha}}u^{\alpha-1}e^{-\frac{u}{\beta}} \tag{A.4}$$

with α and β being the shape and scale parameters. Similarly, by the CLT, we can obtain that

$$\left(e_{l,k} - \hat{m}_{e_l}\right)|\mathcal{H}_0 \sim \mathcal{N}\left(0, \frac{K-1}{K}\sigma_n^4\right). \tag{A.5}$$

Thus, we have

$$K\hat{v}_{e_l}^2|\mathcal{H}_0 \sim \text{Gamma}\left(\frac{K-1}{2}, \frac{2(K-1)}{K}\sigma_n^4\right), \tag{A.6}$$

and then

$$\hat{v}_{e_l}^2|\mathcal{H}_0 \sim \text{Gamma}\left(\frac{K-1}{2}, \frac{2(K-1)}{K^2}\sigma_n^4\right). \tag{A.7}$$

By noting that the elements in $\{\hat{v}_{e_l}^2\}$ are i.i.d., we can have

$$\sum_{l=1}^{L}\hat{v}_{e_l}^2|\mathcal{H}_0 \sim \text{Gamma}\left(\frac{L(K-1)}{2}, \frac{2(K-1)}{K^2}\sigma_n^4\right). \tag{A.8}$$

Let

$$\alpha_1 = \frac{L-1}{2}, \tag{A.9}$$

$$\beta_1^{\mathcal{H}_0} = \frac{2(L-1)}{LK}, \tag{A.10}$$

$$\alpha_2 = \frac{L(K-1)}{2} \tag{A.11}$$

and

$$\beta_2^{\mathcal{H}_0} = \frac{2(K-1)}{K^2}. \tag{A.12}$$

With (A.3) and (A.8), it can be obtained from [37] that the PDF of T_{proposed} under $\mathcal{H}_0$ is approximately given by (A.13), shown at the bottom of this page.

With sufficiently large L and K, it is given that

$$\beta_1^{\mathcal{H}_0} \approx \beta_2^{\mathcal{H}_0}. \tag{A.14}$$

Then, T_{proposed} under $\mathcal{H}_0$ approximately follows beta distribution as

$$T_{\text{proposed}}|\mathcal{H}_0 \sim \text{Beta}\left(\frac{L-1}{2}, \frac{L(K-1)}{2}\right). \tag{A.15}$$

□

$$f_{T_{\text{proposed}}|\mathcal{H}_0}(u) = \frac{\left(\frac{\beta_2^{\mathcal{H}_0}}{\beta_1^{\mathcal{H}_0}+\beta_2^{\mathcal{H}_0}}\right)^{\alpha_1}\left(\frac{\beta_1^{\mathcal{H}_0}}{\beta_1^{\mathcal{H}_0}+\beta_2^{\mathcal{H}_0}}\right)^{\alpha_2}u^{\alpha_1-1}(1-u)^{\alpha_2-1}}{B(\alpha_1,\alpha_2)\left(\frac{\beta_2^{\mathcal{H}_0}u}{\beta_1^{\mathcal{H}_0}+\beta_2^{\mathcal{H}_0}} + \frac{\beta_1^{\mathcal{H}_0}(1-u)}{\beta_1^{\mathcal{H}_0}+\beta_2^{\mathcal{H}_0}}\right)^{\alpha_1+\alpha_2}}, 0 \le u \le 1. \tag{A.13}$$

APPENDIX B
PROOF OF PROPOSITION 3

It is difficult to obtain an exact distribution for the proposed detector under $\mathcal{H}_1$. In the following, we derive an approximate but analytical result with sufficiently large K and L. Under $\mathcal{H}_1$,

$$e_{l,k} = g_l|h_l(k)s_l(k)|^2 + |n_l(k)|^2 + 2\sqrt{g_l}\mathbb{R}(h_l(k)s_l(k)n_l^*(k)). \tag{B.1}$$

Hence, the power at the lth SU is given by

$$\hat{m}_{e_l} = \frac{g_l}{K}\sum_{k=1}^{K}|h_l(k)s_l(k)|^2 + \frac{1}{K}\sum_{k=1}^{K}|n_l(k)|^2 + \frac{2\sqrt{g_l}}{K}\sum_{k=1}^{K}\mathbb{R}(h_l(k)s_l(k)n_l^*(k)). \tag{B.2}$$

It can be obtained that $\mathbb{R}(h_l(k)s_l(k)n_l^*(k))$ is symmetrically distributed, and so

$$\frac{1}{K}\sum_{k=1}^{K}\mathbb{R}(h_l(k)s_l(k)n_l^*(k)) \approx 0 \tag{B.3}$$

for a sufficiently large K. In addition, for the sufficiently large K,

$$\frac{1}{K}\sum_{k=1}^{K}|n_l(k)|^2 \approx \sigma_n^2 \tag{B.4}$$

and

$$\frac{1}{K}\sum_{k=1}^{K}|h_l(k)s_l(k)|^2 \approx \mathbb{E}[|h_l(k)|^2]\sigma_s^2 = \Omega\sigma_s^2 \tag{B.5}$$

Then

$$\hat{m}_{e_l} \approx g_l\Omega\sigma_s^2 + \sigma_n^2 \tag{B.6}$$

and

$$\hat{m}_{e_l} - \frac{1}{L}\sum_{l=1}^{L}\hat{m}_{e_l} \approx \left(\tfrac{(L-1)}{L}g_l - \tfrac{1}{L}\sum_{l'\neq l,l'=1}^{L}g_{l'}\right)\Omega\sigma_s^2. \tag{B.7}$$

By the CLT, for a sufficiently large L, we have

$$\hat{m}_{e_l} - \frac{1}{L}\sum_{l=1}^{L}\hat{m}_{e_l} \sim \mathcal{N}\left(0, \frac{L-1}{L}\mathbb{V}[g_l]\Omega^2\sigma_s^4\right) \tag{B.8}$$

where

$$\mathbb{V}[g_l] = \left(e^{\sigma^2} - 1\right)e^{2\mu+\sigma^2}. \tag{B.9}$$

Therefore,

$$\sum_{l=1}^{L}\left(\hat{m}_{e_l} - \frac{1}{L}\sum_{l=1}^{L}\hat{m}_{e_l}\right)^2 |\mathcal{H}_1 \sim \text{Gamma}\left(\frac{L-1}{2}, \frac{2(L-1)}{L}\mathbb{V}[g_l]\Omega^2\sigma_s^4\right)0. \tag{B.10}$$

The term $e_{l,k} - \hat{m}_{e_l}$ is given by

$$\begin{aligned} e_{l,k} - \hat{m}_{e_l} &= \frac{(K-1)g_l}{K}|h_l(k)s_l(k)|^2 + \frac{K-1}{K}|n_l(k)|^2 \\ &\quad - \frac{g_l}{K}\sum_{k'\neq k,k'=1}^{K}|h_l(k')s_l(k')|^2 - \frac{1}{K}\sum_{k'\neq k,k'=1}^{K}|n_l(k')|^2 \\ &\quad + \frac{2(K-1)\sqrt{g_l}}{K}\mathbb{R}(h_l(k)s_l(k)n_l^*(k)) \\ &\quad - \frac{2\sqrt{g_l}}{K}\sum_{k'\neq k,k'=1}^{K}\mathbb{R}(h_l(k')s_l(k')n_l^*(k')). \end{aligned} \tag{B.11}$$

By the CLT, $e_{l,k} - \hat{m}_{e_l}$ is approximately Gaussian distributed with mean zero and variance

$$\begin{aligned} \mathbb{V}[e_{l,k} - \hat{m}_{e_l}] = \frac{K-1}{K}(&\mathbb{V}[g_l|h_l(k)s_l(k)|^2] + \sigma_n^4 \\ &+ 4\mathbb{V}[\sqrt{g_l}]\mathbb{V}[h_l(k)]\sigma_s^2\sigma_n^2 \\ &+ 4\mathbb{E}[\sqrt{g_l}]^2\mathbb{V}[h_l(k)]\sigma_s^2\sigma_n^2) \end{aligned} \tag{B.12}$$

where

$$\begin{aligned} \mathbb{V}[g_l|h_l(k)s_l(k)|^2] = \sigma_s^4(&2\mathbb{V}[g_l]\mathbb{V}[|h_l(k)|^2] \\ &+ 2\mathbb{V}[g_l]\mathbb{E}[|h_l(k)|^2]^2 \\ &+ 2\mathbb{E}[g_l]^2\mathbb{V}[|h_l(k)|^2] \\ &+ \mathbb{E}[g_l]^2\mathbb{E}[|h_l(k)|^2]^2), \end{aligned} \tag{B.13}$$

$$\mathbb{E}[g_l] = e^{\mu+\frac{\sigma^2}{2}}, \tag{B.14}$$

$$\mathbb{V}[|h_l(k)|^2] = m\Omega^2, \tag{B.15}$$

$$\begin{aligned} \mathbb{V}[\sqrt{g_l}] &= \mathbb{E}[g_l] - \left(\int_0^{+\infty}\sqrt{u}f_{g_l}(u)du\right)^2 \\ &= e^{\mu+\frac{\sigma^2}{2}} - \left(\int_0^{+\infty}\sqrt{u}f_{g_l}(u)du\right)^2 \end{aligned} \tag{B.16}$$

and

$$\mathbb{V}[h_l(k)] = \mathbb{E}[|h_l(k)|^2] - \mathbb{E}[h_l(k)]^2 = \Omega. \tag{B.17}$$

Then

$$\hat{v}_{e_l}^2|\mathcal{H}_1 \sim \text{Gamma}\left(\frac{K-1}{2}, \frac{2}{K}\mathbb{V}[e_{l,k} - \hat{m}_{e_l}]\right), \tag{B.18}$$

which gives

$$\sum_{l=1}^{L}\hat{v}_{e_l}^2|\mathcal{H}_1 \sim \text{Gamma}\left(\frac{L(K-1)}{2}, \frac{2}{K}\mathbb{V}[e_{l,k} - \hat{m}_{e_l}]\right). \tag{B.19}$$

Let

$$\beta_1^{\mathcal{H}_1} = \frac{2(M-1)}{M}\left(e^{\sigma^2} - 1\right)e^{2\mu+\sigma^2}\Omega^2\sigma_s^4 \tag{B.20}$$

and

$$\beta_2^{\mathcal{H}_1} = \frac{2}{K}\mathbb{V}[e_{l,k} - \hat{m}_{e_l}] \tag{B.21}$$

where $\mathbb{V}[e_{l,k} - \hat{m}_{e_l}]$ is given in (B.12). Then, it can be obtained from [37] that the PDF of T_{proposed} under $\mathcal{H}_1$ is approximately given by (B.22), shown at the top of the next page. It can

$$f_{T_{\text{proposed}}|\mathcal{H}_1}(u) = \frac{\left(\frac{\beta_2^{\mathcal{H}_1}}{\beta_1^{\mathcal{H}_1}+\beta_2^{\mathcal{H}_1}}\right)^{\alpha_1}\left(\frac{\beta_1^{\mathcal{H}_1}}{\beta_1^{\mathcal{H}_1}+\beta_2^{\mathcal{H}_1}}\right)^{\alpha_2} u^{\alpha_1-1}(1-u)^{\alpha_2-1}}{B(\alpha_1,\alpha_2)\left(\frac{\beta_2^{\mathcal{H}_1}u}{\beta_1^{\mathcal{H}_1}+\beta_2^{\mathcal{H}_1}}+\frac{\beta_1^{\mathcal{H}_1}(1-u)}{\beta_1^{\mathcal{H}_1}+\beta_2^{\mathcal{H}_1}}\right)^{\alpha_1+\alpha_2}}, 0 \le u \le 1. \tag{B.22}$$

be further obtained from [38] that the PDF of (B.22) can be approximated by the PDF of Beta (α_1, β_3) where

$$\beta_3 = \alpha_1\left(\frac{1}{m_T} - 1\right) \tag{B.23}$$

with m_T being the mean of $T_{\text{proposed}}|\mathcal{H}_1$. According to [38], m_T is given by

$$m_T = \left(\frac{\beta_2^{\mathcal{H}_1}}{\beta_1^{\mathcal{H}_1}}\right)^{\alpha_1}\frac{B(\alpha_2,\alpha_1+1)}{B(\alpha_1,\alpha_2)} \times {}_2F_1\left(\alpha_1+\alpha_2,\alpha_1+1;\alpha_1+\alpha_2+1;1-\frac{\beta_2^{\mathcal{H}_1}}{\beta_1^{\mathcal{H}_1}}\right) \tag{B.24}$$

where ${}_2F_1(\cdot,\cdot;\cdot;\cdot)$ denotes the hypergeometric function [39]. Thus, T_{proposed} under $\mathcal{H}_1$ approximately follows a beta distribution as

$$T_{\text{proposed}}|\mathcal{H}_1 \sim \text{Beta}(\alpha_1, \beta_3). \tag{B.25}$$

□

REFERENCES

[1] S. K. Sharma, T. E. Bogale, S. Chatzinotas, B. Ottersten, L. B. Le, and X. Wang, "Cognitive radio techniques under practical imperfections: A survey," *IEEE Commun. Surveys Tuts.*, vol. 17, no. 4, pp. 1858–1884, 4th Quart., 2015.

[2] T. Yucek and H. Arslan, "A survey of spectrum sensing algorithms for cognitive radio applications," *IEEE Commun. Surveys Tuts.*, vol. 11, no. 1, pp. 116–130, 1st Quart., 2009.

[3] S. Gurugopinath, R. Muralishankar, and H. N. Shankar, "Differential entropy-driven spectrum sensing under generalized Gaussian noise," *IEEE Commun. Lett.*, vol. 20, no. 7, pp. 1321–1324, Jul. 2016.

[4] Q. Zou, S. Zheng, and A. H. Sayed, "Cooperative sensing via sequential detection," *IEEE Trans. Signal Process.*, vol. 58, no. 12, pp. 6266–6283, Dec. 2010.

[5] A. Montazeri, J. Haddadnia, and S. H. Safavi, "Fuzzy hypothesis testing for cooperative sequential spectrum sensing under noise uncertainty," *IEEE Commun. Lett.*, vol. 20, no. 12, pp. 2542–2545, Dec. 2016.

[6] I. F. Akyildiz, B. F. Lo, and R. Balakrishnan, "Cooperative spectrum sensing in cognitive radio networks: A survey," *Phys. Commun.*, vol. 4, no. 1, pp. 40–62, Mar. 2011.

[7] A. Ali and W. Hamouda, "Advances on spectrum sensing for cognitive radio networks: Theory and applications," *IEEE Commun. Surveys Tuts.*, vol. 19, no. 2, pp. 1277–1304, 2nd Quart., 2017.

[8] E. Chatziantoniou, B. Allen, V. Velisavljevic, P. Karadimas, and J. Coon, "Energy detection based spectrum sensing over two-wave with diffuse power fading channels," *IEEE Trans. Veh. Technol.*, vol. 66, no. 1, pp. 868–874, Jan. 2017.

[9] C. Liu, M. Li, and M. L. Jin, "Blind energy-based detection for spatial spectrum sensing," *IEEE Wireless Commun. Lett.*, vol. 4, no. 1, pp. 98–101, Feb. 2015.

[10] J. Lunden, V. Koivunen, A. Huttunen, and H. V. Poor, "Collaborative cyclostationary spectrum sensing for cognitive radio systems," *IEEE Trans. Signal Process.*, vol. 57, no. 11, pp. 4182–4195, Nov. 2009.

[11] A. M. Elzanati, M. F. Abdelkader, K. G. Seddik, and A. M. Ghuniem, "Collaborative compressive spectrum sensing using Kronecker sparsifying basis," in *Proc. IEEE WCNC*, Apr. 2013, pp. 2902–2907.

[12] Z. Lu, Y. Ma, P. Cheraghi, and R. Tafazolli, "Novel pilot-assisted spectrum sensing for OFDM systems by exploiting statistical difference between subcarriers," *IEEE Trans. Commun.*, vol. 61, no. 4, pp. 1264–1276, Apr. 2013.

[13] S. Chaudhari, V. Koivunen, and H. V. Poor, "Autocorrelation-based decentralized sequential detection of OFDM signals in cognitive radios," *IEEE Trans. Signal Process.*, vol. 57, no. 7, pp. 2690–2700, Jul. 2009.

[14] M. Jin, Q. Guo, J. Xi, Y. Li, and Y. Li, "On spectrum sensing of OFDM signals at low SNR: New detectors and asymptotic performance," *IEEE Trans. Signal Process.*, vol. 65, no. 12, pp. 3218–3233, Jun. 2017.

[15] Y. Zeng and Y.-C. Liang, "Spectrum-sensing algorithms for cognitive radio based on statistical covariances," *IEEE Trans. Veh. Technol.*, vol. 58, no. 4, pp. 1804–1815, May 2009.

[16] M. Jin, Y. Li, and H.-G. Ryu, "On the performance of covariance based spectrum sensing for cognitive radio," *IEEE Trans.Signal Process.*, vol. 60, no. 7, pp. 3670–3682, Jul. 2012.

[17] Y. Zeng and Y.-C. Liang, "Eigenvalue-based spectrum sensing algorithms for cognitive radio," *IEEE Trans. Commun.*, vol. 57, no. 6, pp. 1784–1793, Jun. 2009.

[18] T. J. Lim, R. Zhang, Y. C. Liang, and Y. Zeng, "GLRT-based spectrum sensing for cognitive radio," in *Proc. IEEE Global Telecommun. Conf.*, Nov./Dec. 2008, pp. 1–5.

[19] P. Wang, J. Fang, N. Han, and H. Li, "Multiantenna-assisted spectrum sensing for cognitive radio," *IEEE Trans. Veh. Technol.*, vol. 59, no. 4, pp. 1791–1800, May 2010.

[20] G. Yang *et al.*, "Cooperative spectrum sensing in heterogeneous cognitive radio networks based on normalized energy detection," *IEEE Trans. Veh. Technol.*, vol. 65, no. 3, pp. 1452–1463, Mar. 2016.

[21] H. A. Shah, M. Usman, and I. Koo, "Bioinformatics-inspired quantized hard combination-based abnormality detection for cooperative spectrum sensing in cognitive radio networks," *IEEE Sensors J.*, vol. 15, no. 4, pp. 2324–2334, Apr. 2015.

[22] J. So and W. Sung, "Group-based multibit cooperative spectrum sensing for cognitive radio networks," *IEEE Trans. Veh. Technol.*, vol. 65, no. 12, pp. 10193–10198, Dec. 2016.

[23] Z. Quan, S. Cui, and A. H. Sayed, "Optimal linear cooperation for spectrum sensing in cognitive radio networks," *IEEE J. Sel. Topics Signal Process.*, vol. 2, no. 1, pp. 28–40, Feb. 2008.

[24] J. Ma, G. Zhao, and Y. Li, "Soft combination and detection for cooperative spectrum sensing in cognitive radio networks," *IEEE Trans. Wireless Commun.*, vol. 7, no. 11, pp. 4502–4507, Nov. 2008.

[25] D. Hamza, S. Aissa, and G. Aniba, "Equal gain combining for cooperative spectrum sensing in cognitive radio networks," *IEEE Trans. Wireless Commun.*, vol. 13, no. 8, pp. 4334–4345, Aug. 2014.

[26] V. G. Chavali and C. R. C. M. da Silva, "Collaborative spectrum sensing based on a new SNR estimation and energy combining method," *IEEE Trans. Veh. Technol.*, vol. 60, no. 8, pp. 4024–4029, Oct. 2011.

[27] N. Reisi, S. Gazor, and M. Ahmadian, "Distributed cooperative spectrum sensing in mixture of large and small scale fading channels," *IEEE Trans. Wireless Commun.*, vol. 12, no. 11, pp. 5406–5412, Nov. 2013.

[28] C. Wonseok, S. Moon-Gun, A. Jaeha, and I. Gi-Hong, "Soft combining for cooperative spectrum sensing over fast-fading channels," *IEEE Commun. Lett.*, vol. 18, no. 2, pp. 193–196, Feb. 2014.

[29] H. Guo, N. Reisi, W. Jiang, and W. Luo, "Soft combination for cooperative spectrum sensing in fading channels," *IEEE Access*, vol. 5, pp. 975–986, 2017.

[30] H. Guo, W. Jiang, and W. Luo, "Linear soft combination for cooperative spectrum sensing in cognitive radio networks," *IEEE Commun. Lett.*, vol. 21, no. 7, pp. 1573–1576, Jul. 2017.

[31] A. Mariani, A. Giorgetti, and M. Chiani, "Effects of noise power estimation on energy detection for cognitive radio applications," *IEEE Trans. Commun.*, vol. 59, no. 12, pp. 3410–3420, Dec. 2011.

[32] N. C. Beaulieu, A. A. Abu-Dayya, and P. J. McLane, "Estimating the distribution of a sum of independent lognormal random variables," *IEEE Trans. Commun.*, vol. 43, no. 12, pp. 2869–2873, Dec. 1995.

[33] D. Quade, "Using weighted rankings in the analysis of complete blocks with additive block effects," *J. Amer. Statist. Assoc.*, vol. 74, no. 367, pp. 680–683, Dec. 1979.
[34] P. Sprent and N. C. Smeeton, *Applied Nonparametric Statistical Methods*, 3rd ed. Boca Raton, FL, USA: CRC Press, 2000.
[35] J. H. Skillings, "Adaptively combining independent Jonckheere statistics in a randomized block design with unequal scales," *Commun. Statist.–Theory Methods*, vol. 7, no. 11, pp. 1027–1039, 1978.
[36] D. R. Cox, "A note on the asymptotic distribution of range," *Biometrika*, vol. 35, nos. 3–4, pp. 310–315, Dec. 1948.
[37] K. O. Bowman, L. R. Shenton, and P. C. Gailey, "Distribution of the ratio of gamma variates," *Commun. Statist.-Simul. Comput.*, vol. 27, no. 1, pp. 1–19, 1998.
[38] R. Kwan and C. Leung, "Gamma variate ratio distribution with application to CDMA performance analysis," in *Proc. IEEE/Sarnoff Symp. Adv. Wired Wireless Commun.*, Princeton, NJ, USA, Apr. 2005, pp. 188–191.
[39] I. S. Gradshteyn and I. M. Ryzhik, *Table of Integrals, Series, and Products*, 7th ed. New York, NY, USA: Academic, 2007.
[40] X. Hu, X.-Z. Xie, T. Song, and W. Lei, "An algorithm for energy detection based on noise variance estimation under noise uncertainty," in *Proc. IEEE 14th Int. Conf. Commun. Technol. (ICCT)*, Nov. 2012, pp. 1345–1349.

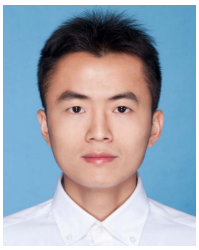

Jingwen Tong received the B.E. degree in electrical engineering from China Jiliang University, Hangzhou, China, in 2015. He is currently pursuing the M.S. degree in electrical engineering with Ningbo University, Ningbo, China. His current research interests include cognitive radio and localization.

Ming Jin received the B.E. and Ph.D. degrees in electrical engineering from Xidian University, Xi'an, China, in 2005 and 2010, respectively.

He is currently an Associate Professor with Ningbo University, Ningbo, China. His current research interests include signal detection and localization.

Qinghua Guo (S'07–M'08) received the B.E. degree in electronic engineering and the M.E. degree in signal and information processing from Xidian University, Xi'an China, in 2001 and 2004, respectively, and the Ph.D. degree in electronic engineering from the City University of Hong Kong, Kowloon, Hong Kong, in 2008.

He is currently a Senior Lecturer with the School of Electrical, Computer and Telecommunications Engineering, University of Wollongong, Wollongong, NSW, Australia, and an Adjunct Associate Professor with the School of Electrical, Electronic and Computer Engineering, The University of Western Australia, Perth, WA, Australia. His research interests include signal processing and telecommunications. He was a recipient of the Discovery Early Career Researcher Award from the Australian Research Council.

Youming Li received the B.S. degree in computational mathematics from Lanzhou University, Lanzhou, China, in 1985, the M.S. degree in computational mathematics from Xi'an Jiaotong University, Xi'an, China, in 1988, and the Ph.D. degree in electrical engineering from Xidian University, Xi'an, in 1995. From 1988 to 1998, he was with the Department of Applied Mathematics, Xidian University, where he was an Associate Professor. From 1999 to 2000, he was a Research Fellow with the School of Electrical and Electronic Engineering, Nanyang Technological University, Singapore. From 2001 to 2003, he was with DSO National Laboratories, Singapore. In 2004, he was a Research Fellow with the School of Engineering, Bar-Ilan University, Israel. Since 2005, he has been with the Faculty of Electrical Engineering and Computer Science, Ningbo University, where he is currently the Vice Dean and a Professor. His research interests include statistical signal processing and its application in communications, cognitive radio, and underwater acoustic communications.